Ultrasonics Sonochemistry 86 (2022) 106029

Contents lists available at ScienceDirect

Ultrasonics Sonochemistry

journal homepage: www.elsevier.com/locate/ultson

Sonosynthesis of nanobiotics with antimicrobial and antioxidant properties

Haiyan Zhu [a], Qinghui Wen [b], Sukhvir Kaur Bhangu [c], Muthupandian Ashokkumar [a,*], Francesca Cavalieri [c,d,*]

[a] School of Chemistry, The University of Melbourne, Parkville, Melbourne, Victoria 3010, Australia
[b] School of Food Science and Engineering, South China University of Technology, Guangzhou 510641, China
[c] School of Science, RMIT University, Victoria 3000, Australia
[d] Department of Chemical Sciences and Technology, University of Rome Tor Vergata, Via della Ricerca Scientifica 1, 00133 Rome, Italy

ARTICLE INFO

Keywords:
Acoustic cavitation
Doxycycline
Nanoparticles
Antimicrobial
Antioxidant

ABSTRACT

Transforming small-molecule antibiotics into carrier-free nanoantibiotics represents an opportunity for developing new multifunctional therapeutic agents. In this study, we demonstrate that acoustic cavitation produced by high-frequency ultrasound transforms the antibiotic doxycycline into carrier-free nanobiotics. Upon sonication for 1 h at 10–15 W cm^{-3}, doxycycline molecules underwent hydroxylation and dimerization processes to ultimately self-assemble into nanoparticles of ~100–200 nm in size. Micrometer sized particles can be also obtained by increasing the acoustic power to 20 W cm^{-3}. The nanodrugs exhibited antioxidant properties, along with antimicrobial activity against both Gram-positive (*S. aureus)* and Gram-negative *(E. coli)* bacterial strains. Our results highlight the feasibility of the ultrasound-based approach for engineering drug molecules into a nanosized formulation with controlled and multiple bio-functionalities.

1. Introduction

Tetracyclines are a class of broad-spectrum antibiotics isolated from *Streptomyces aureofaciens* with tetracene ring structures, which have been widely studied and used since their discovery [1,2]. Among them, doxycycline (Doxy) is the most commonly prescribed semi-synthetic tetracycline which was FDA-approved in 1967 [3,4]. The action mechanism of Doxy is based on the inhibition of protein biosynthesis by preventing aminoacyl-tRNA from binding to the 30S ribosomal acceptor (A) site [5]. However, the broad use and the improper administration of Doxy have caused bacteria to develop resistance against it [5]. Besides, Doxy can also cause side effects such as gastrointestinal irritation and local inflammation in patients that require high doses to achieve therapeutic efficiency due to antibiotic resistance. The development of chemical modifications of antibiotic scaffolds or the synthesis of new high efficacy antibiotics remain key to overcoming the problem of antibiotic resistance.

To combat the antibiotic resistance, nanodrugs have emerged as a promising solution by incorporating antibiotic molecules into nanoscale carriers to control biodistribution and pharmacokinetics [6]. Many studies have reported that loading doxycycline into nanocarriers (i.e. chitosan, polymers, lipids, metals) can improve the antimicrobial activity of doxycycline [7–11]. Although the nanocarriers loaded with antibiotics can decrease the dose required to reduce the bacterial resistance, safety issues such as cytotoxicity, biocompatibility, biodegradability and immunological activity can be raised by the nanocarrier chemical components [12]. In addition, the production of organic or inorganic nanocarriers typically requires the use of toxic organic solvents (N,N-dimethylformamide, chloroform and dimethyl sulfoxide), initiators (azobis (isobutyronitrile) and potassium persulphate), cross-linking agents (glutaraldehyde and isocyanates) and surfactants (cetyltrimethylammonium bromide).

A better way to design antibiotic nanodrug platforms is to fabricate nanodrugs solely made of antibiotic molecules using a green approach. Unlike small drugs that are rapidly metabolized and excreted by the body, nanodrug particles enable the slow release of the therapeutic agent. This may prolong the activity of the antibiotics and minimize their side effects. Compared to the aforementioned systems, nanodrugs entirely composed of drug molecules carry a higher dose of active ingredients. The fabrication of such carrier-free nanodrugs must be also scalable and economically feasible.

Recently, ultrasound has emerged as a novel and eco-friendly technique for nanomaterial synthesis in organic, inorganic and biomedical fields [13–19]. Due to the lack of availability of large-scale ultrasonic

* Corresponding authors at: Applied Chemistry and Environmental Science, RMIT, Melbourne, Australia (F. Cavalieri).
E-mail addresses: masho@unimelb.edu.au (M. Ashokkumar), francesca.cavalieri@rmit.edu.au (F. Cavalieri).

https://doi.org/10.1016/j.ultsonch.2022.106029
Received 2 March 2022; Received in revised form 30 March 2022; Accepted 31 March 2022
Available online 7 May 2022

reactors, progressing ultrasonic techniques into industrial scale processes remains a big challenge [20]. Based on laboratory scale reactions, it has been found that acoustic cavitation derived from sound waves can promote chemical modification, polymerization and self-assembly of phenolic molecules into nanoparticles without using external chemical agents [14,21–23]. Bhangu et al. have reported the synthesis of a carrier-free nanodrug made from non-selective anthracycline doxorubicin into a tumour selective drug nanoparticle by using high-frequency ultrasound [24]. It was demonstrated that the oscillating surface of acoustic cavitation bubbles acts as a catalytic binding site, inducing self-assembly of modified molecules at transient gas-liquid interfaces as a result of high local concentration and strong intermolecular interactions upon bubble implosion. In addition, previous studies also highlighted that the dynamic behaviour and lifetime (0.3 ~ 0.1 ms) of bubbles are crucial to allow sufficient modified molecules to diffuse at gas-liquid interfaces before bubble implosion and showed that 300–500 kHz is the optimal ultrasound range to generate high yields of radicals (•OH) [22,25,26].

We reasoned that doxycycline is a phenolic molecule, composed of four aromatic rings, which is likely responsive to the high concentration of radicals generated by high frequency ultrasound. In this study, we investigated the transformation of Doxy into doxycycline nanoparticles (DoxyNPs) using 490 kHz ultrasound and elucidated the mechanism of sono-assembling. We show that the size and morphology can be finely controlled by tuning ultrasound power. The obtained nanodrug maintains antimicrobial functionality and exhibits excellent antioxidant activity. This study paves the way to a possible future application of chemical modified Doxy and DoxyNPs as nanobiotics to overcome antibacterial resistance [27].

2. Experimental details

2.1. Materials

Doxycycline monohydrate, dimethyl sulfoxide (DMSO > 99.9%) and hydrochloric acid (HCl) were purchased from Sigma-Aldrich (St. Louis, MO, USA). HPLC grade methanol, acetonitrile and trifluoroacetic acid (TFA) were procured from MERCK chemicals (Darmstadt, Germany). 2,2-Diphenyl-1-picrylhydrazyl (free radical, 95%) was purchased from Alfa Aesar (UK). Potassium iodide (KI), sodium hydroxide (NaOH), ammonium molybdate tetrahydrate ($(NH_4)_6Mo_7O_{24}{\cdot}4H_2O$) and potassium hydrogen phthalate ($C_8H_5KO_4$) were purchased from Sigma. The strains of *S. aureus* ATCC 25923 and *E. coli* ATCC 35150 were provided by the Microbial Culture Collection Center of Guangdong Institute of Microbiology (Guangzhou, China) and stored at −80 °C in tryptic soy broth (TSB) containing 25% (v/v) of glycerol. Fluorescence probe NHS ester Alexa Fluro 633 was obtained from Invitrogen™. All solutions were prepared in high purity water with a resistivity of 18.2 MΩ·cm at 25 °C from an inline Millipore RiOs/Origin system.

2.2. Sonochemical synthesis of DoxyNPs

An ELAC Nautik generator paired up with an ultrasonic transducer (T&C Power Conversion,Inc) operating at 490 kHz was used to fabricate doxycycline nanoparticles (DoxyNPs). A solution of doxycycline (1 mg/mL) was obtained by pre-heating the suspension at 55 °C under stirring (600 rpm) for 15 min until doxycycline powder was completely dissolved. A sealed glass vial containing doxycycline solution (5 mL) was placed in a custom-made glass cell with a water jacket connected with a water bath to maintain a constant temperature (37 °C ± 2c°C). The sono-assembly reaction was initiated by applying ultrasound at 9.6, 14.4 and 20 W cm^{-3} measured by calorimetry, respectively. Doxycycline standard solutions were sonicated and studied as a function of sonication time for up to 90 min. The purified nanoparticles were obtained by washing with Milli-Q water for 3 times (centrifuge at 7000 rpm for 10 min).

2.3. Characterization of sonicated doxycycline

2.3.1. Morphology and size distribution

The size and morphologies of DoxyNPs were observed using a scanning electron microscope (FEI Teneo Volume Scope) at an acceleration voltage of 10 keV. The purified DoxyNPs were dropped on a carbon-film copper grid (ProSciTech) until air-dried. Then samples were sputter-coated with a thin gold film for imaging acquisition. For stochastic optical reconstruction microscopy (STORM) imaging DoxyNPs were labelled using NHS ester Alexa Fluro 633 and purified by centrifugation (7000 rpm, 15 min) to remove any excess dye. STORM images were acquired using the N-STORM (Nikon) system equipped with a 100× 1.4NA oil immersion objective (Nikon). By adjusting the focus and the total internal reflection fluorescence imaging angle, a high signal to noise ratio was achieved. 5,000–10,000 frames were acquired sequentially. STORM images were processed from 5000 frames of blinking images, and analysis of the population of nano objects was performed with the STORM module of the NIS Elements Nikon software. The average size of particles was obtained by measuring more than 150 particles from SEM and STORM images. The size distribution and zeta potential were also analyzed by Dynamic Light Scattering (DLS) with a Zetasizer Nano ZS from Malvern Instruments Ltd.

2.3.2. UV–vis and fluorescence spectrum

UV–vis absorption measurements of sonicated samples were carried out with a Carry 50 Bio UV–visible spectrophotometer using a 1.0 cm quartz cuvette. To monitor the reaction, a sonicated solution was taken at different sonication times and diluted accordingly for measurements. Fluorescence spectra were obtained using a Shimadzu RF-5301PC fluorescence spectrophotometer (Shimadzu) equipped with a xenon lamp and 1.0 cm optical length quartz cell. To determine the spectral properties of the final products, the Doxy standards and modified dissolved DoxyNPs were excited at different wavelengths from 340 to 500 nm using a slit width of 5 nm for excitation and 5 nm for emission spectra. Raman peak (water) was subtracted for processing and presenting emission spectrum.

2.3.3. High performance liquid chromatography (HPLC) and mass spectroscopy

Shimadzu SCL-10AVP high-performance liquid chromatography (HPLC) equipped with a LC-10 AT pump, liquid chromatography with a RESTEK column model Ultra AQ C18 5 μm (150 × 4.6 mm) was used to perform HPLC analysis. All chromatograms were generated by LabSolution software (Shimadzu) and all samples were injected 20 μL by SCL-10 AVP injector. The sonicated doxycycline solution was diluted by methanol (1:2) in order to completely dissolve the formed particles. HPLC was carried out at 347 nm (UV detector) using a solvent of 30% acetonitrile and 0.1% TFA with the flow rate set at 1 mL/min.

Perkin Elmer AxION® 2 ToF quadrupole mass spectrometer (Perkin Elmer, Waltham, MA, USA) was used for carrying out mass analysis of the sonicated doxycycline samples. The mixture of 30% acetonitrile and 0.1% TFA was used as eluent.

2.4. Measurement of radical yields and antioxidant activity

The hydrogen peroxide (H_2O_2) and correlated OH radical yield were determined following Weissler method [28]. 0.4 M reagent A (KI + NaOH+($(NH_4)_6Mo_7O_{24}{\cdot}4H_2O$)) and 0.1 M reagent B ($C_8H_5KO_4$) were pre-prepared as reductants. The sonicated water (1 mL) was collected at different sonication times and diluted accordingly, then add to the mixture of reagent A (1 mL) and B (1 mL) and incubate for 1 min before reading the absorbance (Carry on 50 UV–vis) of the solution·H_2O_2 concentration can be represented as OH yields during sonication of water. The concentration of H_2O_2 can be calculated by using the following equation:

$$c = (A/\varepsilon l) \times 3(M) \quad (1)$$

where A: Absorbance value at 351 nm, ε: the molar extinction coefficient: 26400 M^{-1} cm^{-1}, c: concentration of H_2O_2, l: path length of cuvette 1 cm, Dilution factor: 3.

The antioxidant activity of sonicated doxycycline was monitored using 2,2-diphenyl-1-picrylhydrazyl (DPPH) assay [29]. 250 μM DPPH solution was prepared in ethanol and water (1:1). Standard doxycycline solution (0.1 mL) and sonicated samples were added to 3 mL DPPH solution, for incubation. The absorbance was measured by UV–VIS at 520 nm at different incubation times. The percentage of radicals scavenged can be determined using the following equation:

$$\%\ \text{Radical scavenging activity} = [(A_{DPPH} - A_{sample})/A_{DPPH}] \times 100 \quad (2)$$

where A_{DPPH} and A_{sample} are the absorption values for blank DPPH solution (3 mL DPPH + 0.1 mL water) and after the addition of the standard/sonicated sample.

2.5. Antimicrobial study

The strains of *S. aureus* ATCC 25923 and *E. coli* ATCC 35150 were activated by incubating the suspension in a flask containing 50 mL of sterile tryptic soy broth (TSB) at 37 °C for 24 h with gentle shaking (100 rpm). The two bacterial suspensions (*S. aureus* and *E. coli*) were then diluted to 10^5 cfu and aliquoted 3 mL in each sterile test tube. Doxy and DoxyNps were dissolved in DMSO and added into two bacterial suspensions to the final concentration (0–80 μg/mL), respectively. After 24 h incubation at 37 °C, the turbidity of the samples was observed, and the optical density of bacteria was measured by UV–Vis at 600 nm [30]. The minimum inhibitory concentration is determined by the value of absorbance (OD 600), where the OD600 is close to zero and the trend reaches a plateau.

The minimal inhibitory concentration (MIC) was determined by the incubation of early stationary phase *S. aureus* and *E. coli* cells in 0.1% peptone water (w/v) containing dissolved doxycycline and doxycycline nanoparticles (0–80 μg/mL). Then the samples were measured at 600 nm by UV–vis. The absorbance (OD600) was used to determine the turbidity, which is correlated to living bacteria.

3. Results and discussion

3.1. Synthesis and characterization

Doxycycline nanoparticles (DoxyNPs) were first obtained by sonicating 1 mg/mL doxycycline (Doxy) solution for 1 h using a 490 kHz ultrasound setup at 9.6 W cm^{-3} (yield ~64%). The color of sonicated solution turned from pale yellow to dark brown during the sonication process (Fig. S1A). The obtained DoxyNPs were purified by repeated washing and centrifugation steps (Fig. 1A). Control experiments were performed to ensure that the radicals generated by ultrasound and cavitation bubbles were involved in DoxyNPs formation (Fig. S1). The sono-synthesized DoxyNps were labelled with AF 633 dye and visualized with nanoresolution by stochastic optical reconstruction microscopy (STORM) (Fig. 1B). The average size of DoxyNps in the hydrated state was around 223 ± 45 nm (Fig. S2) with a negative charge −31 ± 5 mV as measured by dynamic light scattering and electrophoretic mobility measurements.

To investigate the chemical modification of doxycycline upon sonication, UV–vis absorbance of samples as a function of sonication time was first measured. The acquired absorption spectra of sonicated solutions (Fig. 1C) showed the characteristic absorption peak of untreated doxycycline at 345 nm and a new absorbance band at 390–680 nm. The absorbance intensity at 345 nm decreased while the intensity of the absorption band at the 90–680 nm range increased in line with

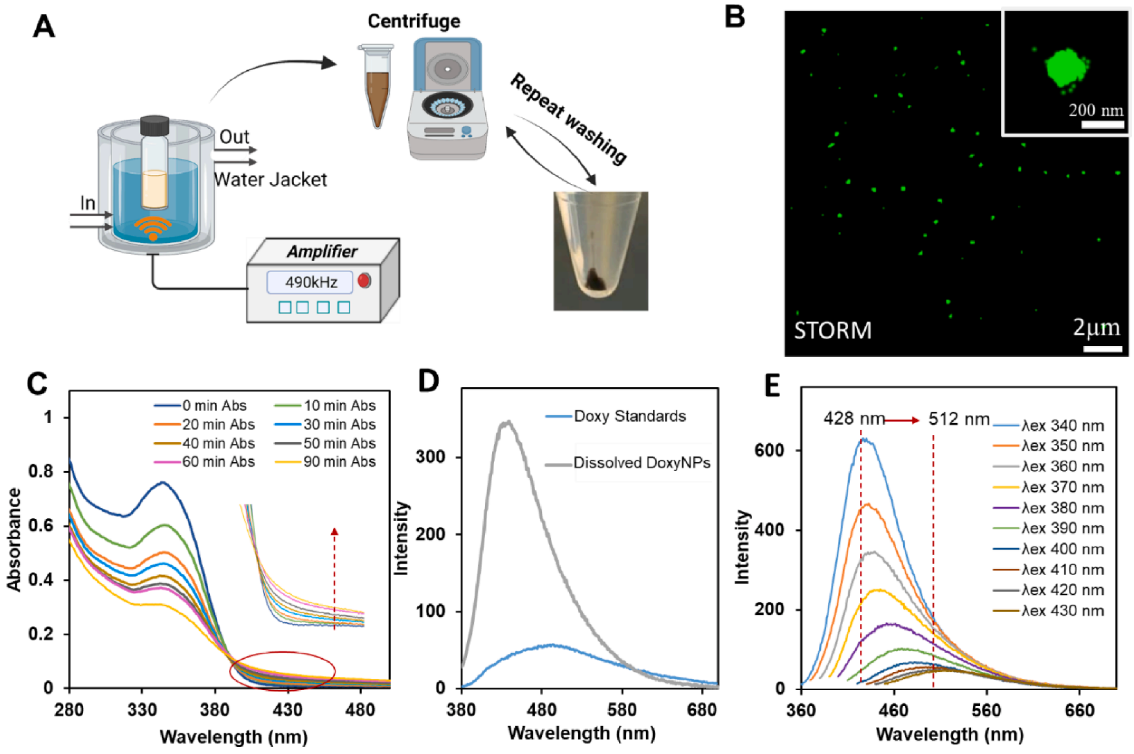

Fig. 1. A) Schematic diagrams show the procedure of sonochemical synthesis of doxycycline nanoparticles using a 490 kHz setup, symbol "))" representing ultrasound; B) Representative STORM imaging of DoxyNps labelled with AF 633 dye; inset showed a magnified view of a single Doxy nanoparticle; C) UV absorbance spectra of sonicated doxycycline solution at different sonication times; D) Emission spectra of Doxy standards and DoxyNPs excited at 360 nm (blue region); E) Dependence of fluorescence emission spectra of the doxycycline nanoparticles (dissolved in PBS 7.4) on the excitation wavelength. The fluorescence emission spectrum was determined by using a slit width of 5 nm for excitation and 5 nm for emission spectra.

sonication time. It is noted that there is an isosbestic point at 390 nm (Fig. 1C), which indicates the presence of two species at equilibrium in the sonicated solutions (i.e., conversion of doxycycline molecules to doxycycline derivatives). This result suggested that the decreasing absorption peak could represent doxycycline conversion while the increasing absorption band could be ascribed to the formation of modified doxycycline species. It has also been noted that the emission peak of modified DoxyNps in the blue region showed much higher intensity than doxycycline solution (Fig. 1D) when samples were excited at 360 nm. This could be attributed to the molecules from modified DoxyNps containing more –OH groups (radical generation from ultrasound) than that of doxycycline standards [21]. To gain further insight into the optical properties, the fluorescence intensity of the modified DoxyNps was measured upon excitation in the 340–430 nm range. It was found that the emission peak was red-shifted from 428 nm to 512 nm, which indicates that multiple species are responsible for the overall fluorescence spectrum (Fig. 1E).

To unveil the chemical composition of DoxyNps and the mechanism of ultrasonic assisted self-assembly, HPLC, ^{1}H NMR and mass spectrometry analysis were performed. The HPLC data (Fig. 2A) indicates a progressive decrease in the intensity of the doxycycline peak (10.2 min retention time) as sonication time increases. In addition, new elution peaks in the range of retention times 1.8–4.2 min, progressively increased as a function of sonication time. These multiple elution peaks present in an earlier retention time indicate that the modified doxycycline is composed of more hydrophilic species. ^{1}H NMR was carried out to further characterize the composition of DoxyNPs (Fig. S3). The peak attributed to the aromatic H8, H9 significantly decreased while the peak at 10.2 ppm attributed to the OH significantly increased. This suggests that the HO• produced by sonication abstract hydrogen from C7, C8, C9, resulting in formation of hydroxylated species. Interestingly, it was found that the peaks of 14($'$C-NH_2), (4$'$CN$(CH_3)_2$), disappeared indicating the cleavage of those groups during sonication to form new derivatives.

Mass spectrometry analysis provided further structural information on the pathway of modified doxycycline fragmentation patterns in the lower and higher *m/z* region were observed (Fig. S4). Possible chemical structures are presented in Fig. 2B and Fig. S4. FITR spectrum and size exclusion chromatogram also confirmed the hydroxylation and higher molecular compounds formation respectively during sonication (Fig. S5). Our data suggests that the mechanism of forming DoxyNps upon sonication undergoes two steps of chemical modification (Fig. 2B). During the oscillation of cavitation bubbles, doxycycline molecules tend to accumulate at the gas-liquid interface. When the bubbles grow to the maximum bubble diameter and start to implode, the generated OH radicals can rapidly attack the surrounding molecules. The radical-mediated oxidation of doxycycline results in: (i) the cleavage of amine/amide moieties to form a new hydroxylated derivative, Monomer (*m/z* 359); (ii) the dimerization reaction to form Dimer (*m/z* 772) by C–C coupling to ultimately self-assemble into DoxyNps (Fig. 2B, Fig. S4).

3.2. Morphological control of particles

Next, we investigated the effect of acoustic power on the morphology

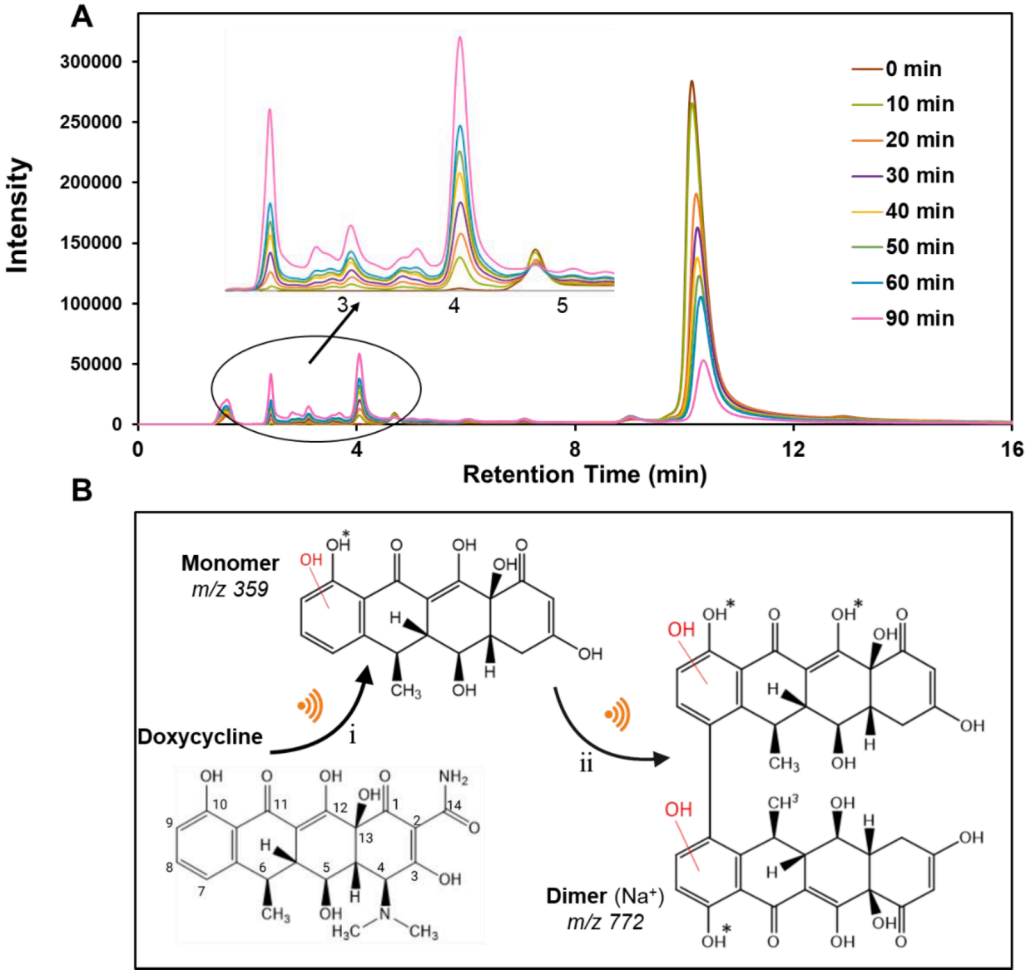

Fig. 2. A) HPLC data of sonicated doxycycline solution as a function of sonication time; B) Proposed chemical structure changes of doxycycline upon sonication (Fig. S4).

of DoxyNPs. It has been reported that the activity level of acoustic cavitation depends on both frequency and applied ultrasound power [31]. In this system, we fixed the ultrasound frequency (490 kHz), while tuning the applied power to study the effect of acoustic power on DoxyNps morphology.

The SEM images (Fig. 3A, B and C) showed the morphologies of DoxyNps after 1 h sonication using 490 kHz ultrasound at different applied power: 9.6 W cm^{-3} (low), 14.4 W cm^{-3} (medium) and 20 W cm^{-3} (high) sonication. The average sizes of obtained particles measured from SEM images is 177 ± 45 nm, 115 ± 20 nm and 1298 ± 500 nm after low, medium and high power sonication, respectively. Interestingly, the hydrodynamic diameters of DoxyNps obtained at the three applied power values measured by DLS (Fig. 3D) are approximately 223 ± 15 nm, 178 ± 16 nm and 5 ± 2 μm, respectively. These values are much larger than that of those measured from SEM images. This indicates that the DoxyNps are highly hydrated and the self-assembly of the modified doxycycline results in the formation of a hydrated physical network stabilized by hydrogen bonds and π–π interaction between the chemically modified Doxy molecules.

It should be noted that the particle size decreased with increasing sonication power from 9.6 to 14.4 W cm^{-3}, while the size of particle significantly increases at 20 W cm^{-3}. The effect of ultrasound power on the size of nanoparticles and nanocrystals probably could be explained by the "nuclei-growth" theory (Fig. 4) [32,33]. The nuclei sites are affected by the amount of active acoustic cavitation [33]. It is known that acoustic cavitation is observed in water when negative pressure in the rarefaction phase of an acoustic wave reaches a certain threshold value. With increasing power, the acoustic cavitation activity is known to be enhanced because bubbles are exposed to greater pressures [34]. It has been reported that a higher amplitude (higher power) might increase the number of active cavitation bubbles and consequently the rate of nucleation for nanoparticles [33,34]. The more nuclei sites formed at an early stage of reaction the less molecules could be distributed surrounding a single nuclei site. Therefore, a higher nucleation rate would lead to a reduction in the size of nanoparticles as the rate of nucleation and radius are inversely related to each other.

Based on this assumption, a reduction in the size of DoxyNPs is expected by increasing the power from 9.6 to 14.4 W cm-3 (Fig. 3 A and B). However, an opposite effect was observed at 20 W cm-3. The formation of micro-size particles indicates that less nuclei sites were formed. Though the number of cavitation bubbles could be high upon 20 W cm^{-3} sonication, some bubbles can collide and merge to form larger radius bubbles (Fig. 4). The buoyancy of such larger size bubbles caused less active acoustic cavitation in water (Fig. S6), resulting in less nuclei sites and more heterogeneous and polydisperse samples (Fig. 3C). Overall, these results indicate that the morphology of sono-assembled doxycycline particles can be affected by the number of active cavitation bubbles, which can be controlled by tuning the applied ultrasonic power.

3.3. *Bio-functionalities of DoxyNPs*

Doxycycline has been widely used as a broad-spectrum antibiotic to treat or prevent bacterial infection. The chemical modification, hydroxylation and dimerization of Doxy during sonication could likely modify its bioactivity. It has been reported that the hydroxylation process upon ultrasonic treatment can enhance the antioxidant properties of the sonicated molecules [21,35]. Therefore, we sought to assess both the antioxidant and antimicrobial properties of sono-assembled DoxyNPs.

A DPPH radical scavenging assay was used to determine antioxidant activity by measuring the decrease of UV absorbance at 520 nm. Fig. 5 shows that the modified DoxyNPs (9.6 and 14.4 W cm^{-3}) exhibit more than 50% and 70% radical scavenging or antioxidant activity compared with the doxycycline standard after 2 min and 15 min incubation, respectively. Though 20 W cm^{-3} samples showed the least activity among three sonicated samples, it still showed more than 40% radical scavenging activity than non-sonicated doxycycline after 15 min incubation. The trend of DPPH radical scavenging activity (medium > low > high power) indicates that the smaller nanoparticles are more active likely because more hydroxyl groups are exposed on the surface of DoxyNPs to scavenge DPPH radicals. This result also confirmed that the

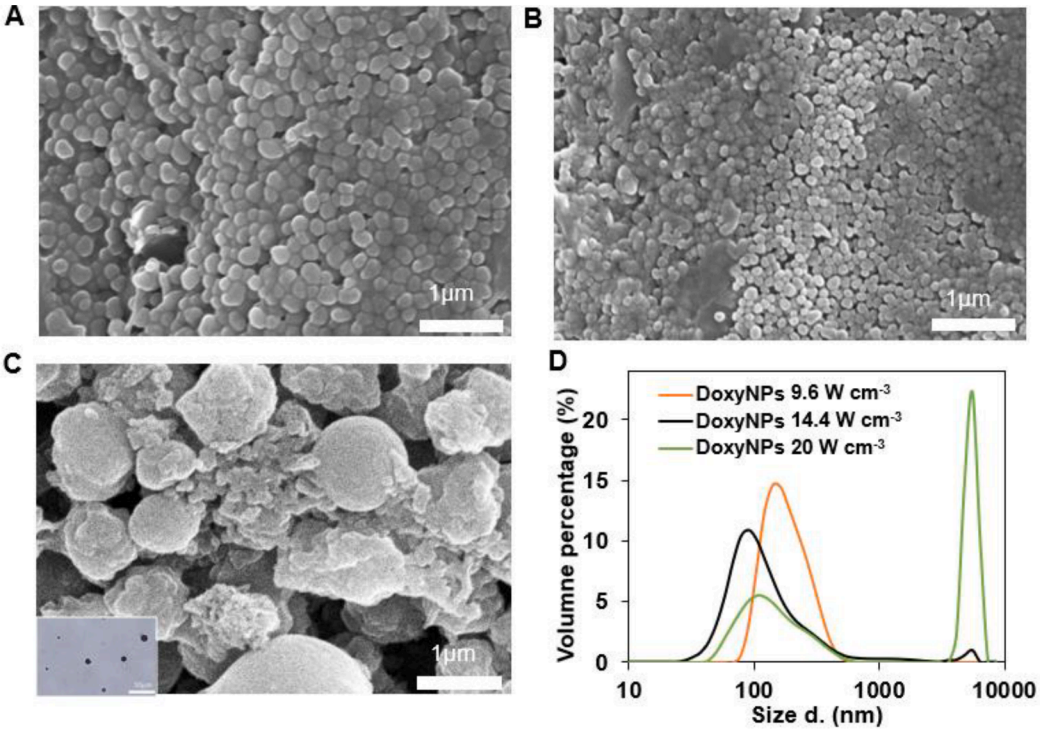

Fig. 3. Controlling of DoxyNPs morphology by tuning ultrasonic power. A, B, C) SEM images of obtained DoxyNPs upon 1 h sonication using 490 kHz ultrasound at 9.6, 14.4 and 20 W cm^{-3} applied power, respectively (inset optical images in C); D) Size distribution of synthesised particles measured by dynamic light scattering instrument (polydisperse size of 20 W cm^{-3} particles: 198 ± 13 nm and 5 ± 2 μm).

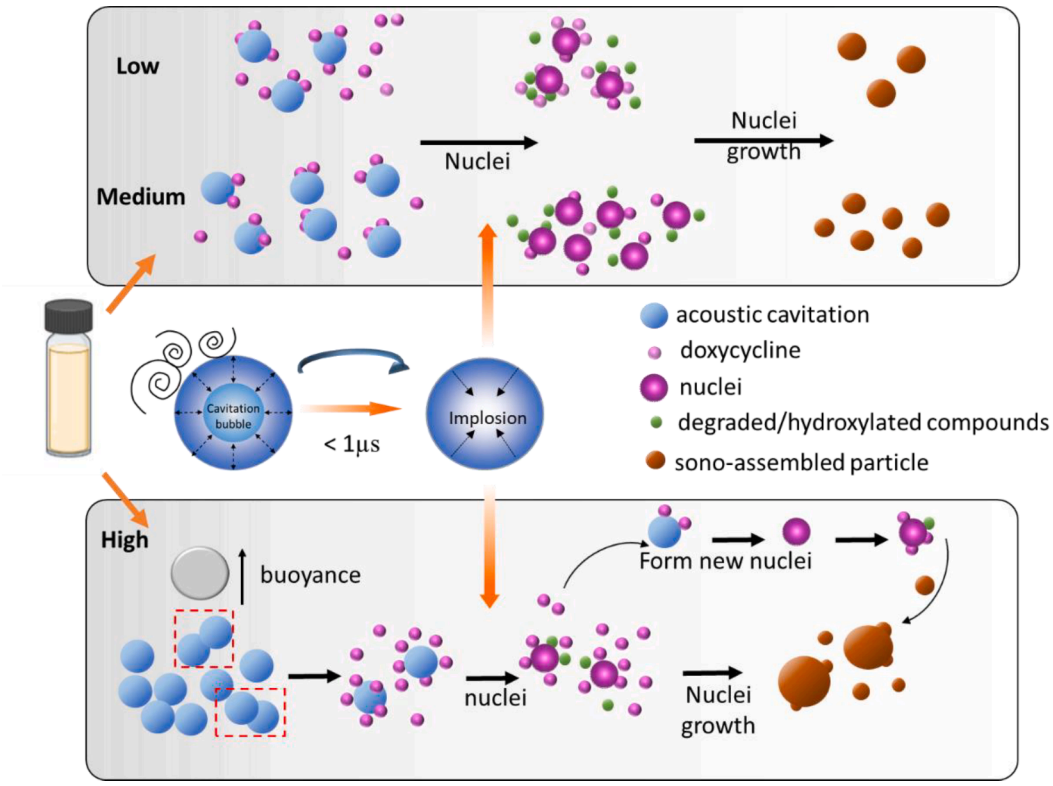

Fig. 4. Schematic diagram of sono-assembled doxycycline nanoparticles upon different ultrasound amplitudes. Low, medium, high represents 9.6, 14.4 and 20 W cm^{-3} applied power, respectively. A single bubble collapses (within 1 μs) can repeat over many acoustic cycles. The diagram presents the process of nuclei formation and growth affected by the acoustic cavitation driven from ultrasound.

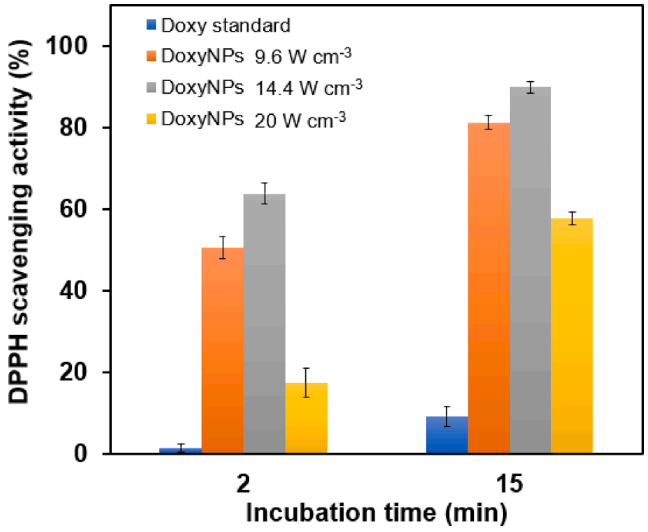

Fig. 5. DPPH scavenging activity of doxycycline standard and sonicated doxycycline (9.6, 14.4 and 20 W cm^{-3} applied power) as a function of incubation time.

doxycycline hydroxylation occurring during the sonication process confers radical scavenging activity to the DoxyNPs. Compared with typical radical scavengers (e.g. ascorbic acid), the obtained DoxyNPs show a similar antioxidant activity (Fig S7).

For assessment of antimicrobial property, cultured Staphylococcus aureus (*S. aureus*) and Escherichia coli (*E. coli)* as gram-positive and negative bacterial strains were incubated with DoxyNPs, at increasing concentrations to determine the minimal inhibitory concentration (MIC) (Fig. 6 A). It is observed that the turbidity of the sample solution of *S. aureus* and *E. coli* treated with DoxyNPs both (Fig. S7 a2 and b2) decreased and showed a trend to be transparent. The turbidity also refers to the absorbance of optical density at 600 nm (OD 600), which reflects bacterial density. The native Doxy show a strong bactericidal activity against both *S. aureus* and *E. coli* at MIC of 5 μg/mL (Fig. S8). When DoxyNPs concentration increased up to 80 μg/mL, the OD 600 value of *S. aureus* had significantly dropped down to nearly zero, while that of the *E. coli* sample was only reduced by about 50% (Fig. 6B). Of note, the antimicrobial activity of DoxyNPs was evaluated after dissolution of the nanoparticles in the media. Our results suggest that the modified Doxy molecules still possess antimicrobial properties and that they are more effective against *S. aureus* than *E. coli*. (Fig. 6B). However, the activity DoxyNPs is 20 times less than that of the original drug. The different antimicrobial effects of DoxyNPs against *S. aureus* (G+) other than *E. coli* (G−). can be ascribed to the differences in cell structure between Gram-positive and Gram-negative bacteria. Compared with gram-positive bacteria, gram-negative bacteria have an additional protective outer layer (Fig. 6C), which could prevent antibiotics from being absorbed in the peptidoglycan layer. Therefore, gram-positive bacteria, those species with thick peptidoglycan layers can easily absorb more antibiotics and consequently be destroyed.

Although the chemical modification of DoxyNPs did not show an improved efficacy in antimicrobial properties, our data suggest that the hydroxylated monomer and dimer structures maintain a significant affinity for the 30S subunit of the ribosome. It is well known that doxycycline acts by binding to the 30S subunit of the ribosome at the A-site, so tRNA with amino acid cannot attach to the blocked A-site, causing the inhibition of protein biosynthesis. Pumping of doxycycline out of the cell before it reaches its binding site (efflux) could cause the decrease of drug binding with A-site, resulting in antibiotic resistance [36]. It has been recently demonstrated that the design of another tetracycline member, sarecycline with long C7 moiety (Fig. S9) is able to overcome the antibiotic resistance. Such extended long C7 moiety could protrude more

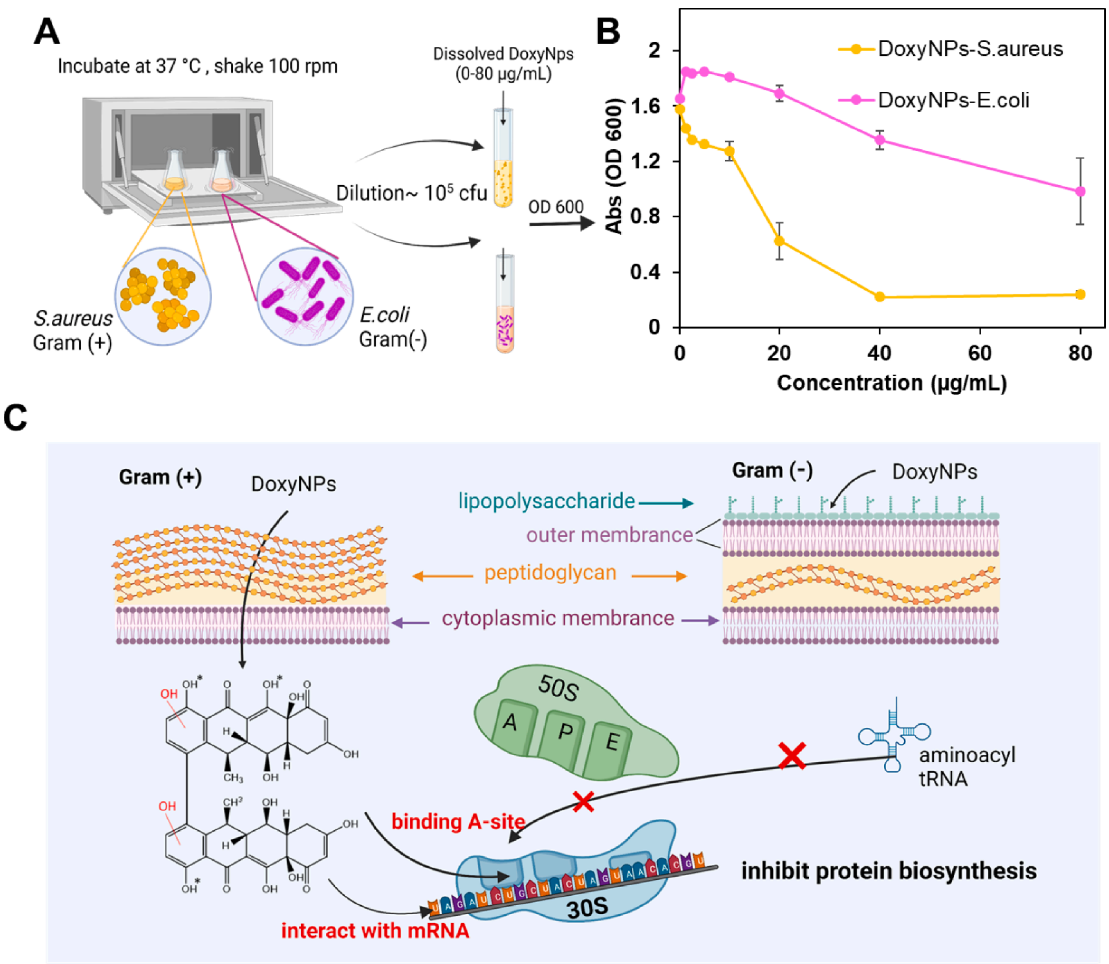

Fig. 6. A) Schematic diagram of antimicrobial test of Doxy standards and DoxyNPs; B) Optical density measurements of bacteria at a wavelength of 600 nm (OD 600) for *S. aureus* and *E. coli* as a function of DoxyNPs concentration; C) Possible mechanism of action of modified DoxyNPs against Gram (+) and Gram (−) bacteria.

antibiotics toward the mRNA binding channel [27]. We reasoned that the modified hydroxylated DoxyNPs molecules may also directly interact with the ribose unit of mRNA, further preventing mRNA sequence from being decoding in to a new protein. (Fig. 6C). A deeper mechanistic insight into the function of DoxyNPs in bacteria will be provided in future studies.

4. Conclusion

A sonochemical strategy for fabricating carrier-free nanodrugs using an existing antibiotic is reported. We showed that a commercial antibiotic, doxycycline undergoes hydroxylation and dimerization processes upon sonication in an aqueous solution to ultimately self-assemble into nanoparticles. The morphology of obtained particles could be finely controlled by tuning the applied ultrasonic powers. The sono-assembled nanodrugs exhibit excellent antioxidant properties, along with antimicrobial activity against both Gram-positive (*S. aureus)* and Gram-negative *(E. coli)* bacteria. Our results provided insight into the feasibility of ultrasonic approaches to engineering drug molecules into biofunctional nanoparticles for improving therapeutic efficacy of commercial drugs.

CRediT authorship contribution statement

Haiyan Zhu: Conceptualization, Investigation, Visualization, Writing – original draft. **Qinghui Wen:** Methodology, Investigation. **Sukhvir Kaur Bhangu:** Conceptualization, Investigation, Methodology. **Muthupandian Ashokkumar:** Conceptualization, Funding acquisition, Project administration, Supervision, Methodology, Writing – review & editing. **Francesca Cavalieri:** Conceptualization, Funding acquisition, Project administration, Supervision, Methodology, Writing – review & editing.

Declaration of Competing Interest

The authors declare the following financial interests/personal relationships which may be considered as potential competing interests: Serving as Guest Editor of the Special Issue on this journal.

Acknowledgements

Miss Haiyan Zhu acknowledges the University of Melbourne for the award of a Melbourne Research Scholarship. This work was performed in part at the Materials Characterisation and Fabrication Platform (MCFP) and Bio21 Ian Holmes imaging Center at The University of Melbourne.

Appendix A. Supplementary data

Supplementary data to this article can be found online at https://doi.org/10.1016/j.ultsonch.2022.106029.

References

[1] E.M. Graber, Treating acne with the tetracycline class of antibiotics: A review, Dermatol. Rev. 2 (6) (2021) 321–330.

[2] E. Campos, J. Branquinho, A.S. Carreira, A. Carvalho, P. Coimbra, P. Ferreira, M. H. Gil, Designing polymeric microparticles for biomedical and industrial applications, Eur. Polym. J. 49 (8) (2013) 2005–2021.

[3] N.E. Holmes, P.G. Charles, Safety and efficacy review of doxycycline, Clin. Med. Therap. 1 (2009) CMT. S2035.

[4] B.A. Cunha, C.M. Sibley, A.M. Ristuccia, Doxycycline, Ther. Drug Monit. 4 (1982) 115–135.

[5] D.P. Eisen, Doxycycline, in: Kucers' the use of antibiotics, CRC Press, 2017, pp. 1204–1229.

[6] J.M.V. Makabenta, A. Nabawy, C.-H. Li, S. Schmidt-Malan, R. Patel, V.M. Rotello, Nanomaterial-based therapeutics for antibiotic-resistant bacterial infections, Nat. Rev. Microbiol. 19 (2021) 23–36.

[7] N.F. Cover, S. Lai-Yuen, A.K. Parsons, A. Kumar, Synergetic effects of doxycycline-loaded chitosan nanoparticles for improving drug delivery and efficacy, Int. J. Nanomed. 7 (2012) 2411.

[8] R. Misra, S.K. Sahoo, Antibacterial activity of doxycycline-loaded nanoparticles, in: Methods in enzymology, Elsevier, 2012, pp. 61–85.

[9] S.M. Hosseini, R. Abbasalipourkabir, F.A. Jalilian, S.S. Asl, A. Farmany, G. Roshanaei, M.R. Arabestani, Doxycycline-encapsulated solid lipid nanoparticles as promising tool against Brucella melitensis enclosed in macrophage: a pharmacodynamics study on J774A. 1 cell line, Antimicrob. Resist. Infect. Control 8 (2019) 1–12.

[10] S.A.R. Kazmi, M.Z. Qureshi, S. Ali, J.-F. Masson, In vitro drug release and biocatalysis from pH-responsive gold nanoparticles synthesized using doxycycline, Langmuir 35 (2019) 16266–16274.

[11] M.B. Haddada, K. Jeannot, J. Spadavecchia, Novel Synthesis and Characterization of Doxycycline-Loaded Gold Nanoparticles: The Golden Doxycycline for Antibacterial Applications, Part. Part. Syst. Char. 36 (2) (2019) 1800395.

[12] J. Szebeni, D. Simberg, Á. González-Fernández, Y. Barenholz, M.A. Dobrovolskaia, Roadmap and strategy for overcoming infusion reactions to nanomedicines, Nat. Nanotechnol. 13 (12) (2018) 1100–1108.

[13] T.G. McKenzie, E. Colombo, Q. Fu, M. Ashokkumar, G.G. Qiao, Sono-RAFT Polymerization in Aqueous Medium, Angew. Chem. Int. Ed. 56 (2017) 12302–12306.

[14] Y. Tao, P.F. Wu, Y.X. Dai, X.T. Luo, S. Manickam, D.D. Li, Y.B. Han, P.L. Show, Bridge between mass transfer behavior and properties of bubbles under two-stage ultrasound-assisted physisorption of polyphenols using macroporous resin, Chem. Eng. J. 436 (2022), 135158.

[15] Z. Gao, H. Zhu, X. Li, P. Zhang, M. Ashokkumar, F. Cavalieri, J. Hao, J. Cui, Sono-polymerization of poly (ethylene glycol)-based nanoparticles for targeted drug delivery, ACS Macro Lett. 8 (10) (2019) 1285–1290.

[16] A. Gedanken, Using sonochemistry for the fabrication of nanomaterials, Ultrason. Sonochem. 11 (2004) 47–55.

[17] S. Bibi, A. Jamil, T. Yasin, M.A. Rafiq, M. Nawaz, G.J. Price, Ultrasound promoted synthesis and properties of chitosan nanocomposites containing carbon nanotubes and silver nanoparticles, Eur. Polym. J. 105 (2018) 297–303.

[18] B.M. Teo, F. Chen, T.A. Hatton, F. Grieser, M. Ashokkumar, Novel one-pot synthesis of magnetite latex nanoparticles by ultrasound irradiation, Langmuir 25 (2009) 2593–2595.

[19] H. Zhu, F. Cavalieri, M. Ashokkumar, Ultrasound-Assisted Synthesis of Cross-Linked Poly (ethylene glycol) Nanostructures with Hydrophobic Core and Hydrophilic Shell, Macromol. Chem. Phys. 219 (2018) 1800353.

[20] M. Ashokkumar, Ultrasonic synthesis of functional materials, in: Ultrasonic Synthesis of Functional Materials, Springer, 2016, pp. 17–40.

[21] S.K. Bhangu, M. Ashokkumar, F. Cavalieri, A simple one-step ultrasonic route to synthesize antioxidant molecules and fluorescent nanoparticles from phenol and phenol-like molecules, ACS Sustain. Chem. Eng. 5 (7) (2017) 6081–6089.

[22] F. Cavalieri, E. Colombo, E. Nicolai, N. Rosato, M. Ashokkumar, Sono-assembly of nanostructures via tyrosine–tyrosine coupling reactions at the interface of acoustic cavitation bubbles, Mater. Horiz. 3 (6) (2016) 563–567.

[23] S.K. Bhangu, R. Singla, E. Colombo, M. Ashokkumar, F. Cavalieri, Sono-transformation of tannic acid into biofunctional ellagic acid micro/nanocrystals with distinct morphologies, Green Chem. 20 (4) (2018) 816–821.

[24] S.K. Bhangu, S. Fernandes, G.L. Beretta, S. Tinelli, M. Cassani, A. Radziwon, M. Wojnilowicz, S. Sarpaki, I. Pilatis, N. Zaffaroni, G. Forte, F. Caruso, M. Ashokkumar, F. Cavalieri, Transforming the Chemical Structure and Bio-Nano Activity of Doxorubicin by Ultrasound for Selective Killing of Cancer Cells, Adv. Mater. 34 (13) (2022) 2107964.

[25] M. Ashokkumar, D. Sunartio, S. Kentish, R. Mawson, L. Simons, K. Vilkhu, C. (. Versteeg, Modification of food ingredients by ultrasound to improve functionality: A preliminary study on a model system, Innov. Food Sci. Emerg. Technol. 9 (2) (2008) 155–160.

[26] S.K. Bhangu, G. Bocchinfuso, M. Ashokkumar, F. Cavalieri, Sound-driven dissipative self-assembly of aromatic biomolecules into functional nanoparticles, Nanoscale Horiz. 5 (3) (2020) 553–563.

[27] Z. Batool, I.B. Lomakin, Y.S. Polikanov, C.G. Bunick, Sarecycline interferes with tRNA accommodation and tethers mRNA to the 70S ribosome, Proc. Natl. Acad. Sci. 117 (34) (2020) 20530–20537.

[28] A. Weissler, Formation of hydrogen peroxide by ultrasonic waves: free radicals, J. Am. Chem. Soc. 81 (5) (1959) 1077–1081.

[29] C.-W. Chen, C.-T. Ho, Antioxidant properties of polyphenols extracted from green and black teas, J. Food Lipids 2 (1) (1995) 35–46.

[30] Q.-H. Wen, R. Wang, S.-Q. Zhao, B.-R. Chen, X.-A. Zeng, Inhibition of Biofilm Formation of Foodborne Staphylococcus aureus by the Citrus Flavonoid Naringenin, Foods 10 (2021) 2614.

[31] M. Ashokkumar, J. Lee, Y. Iida, K. Yasui, T. Kozuka, T. Tuziuti, A. Towata, Spatial distribution of acoustic cavitation bubbles at different ultrasound frequencies, ChemPhysChem 11 (2010) 1680–1684.

[32] W. Li, F.-M. Allioux, J. Lee, M. Ashokkumar, L.F. Dumée, Ultrasound-assisted fabrication of metal nano-porous shells across polymer beads and their catalytic activity for reduction of 4-nitrophenol, Ultrason. Sonochem. 49 (2018) 63–68.

[33] S. Kaur Bhangu, M. Ashokkumar, J. Lee, Ultrasound assisted crystallization of paracetamol: crystal size distribution and polymorph control, Cryst. Growth Des. 16 (4) (2016) 1934–1941.

[34] P. Kanthale, M. Ashokkumar, F. Grieser, Sonoluminescence, sonochemistry (H2O2 yield) and bubble dynamics: frequency and power effects, Ultrason. Sonochem. 15 (2) (2008) 143–150.

[35] A. Golmohamadi, G. Möller, J. Powers, C. Nindo, Effect of ultrasound frequency on antioxidant activity, total phenolic and anthocyanin content of red raspberry puree, Ultrason. Sonochem. 20 (2013) 1316–1323.

[36] M.C. Roberts, Tetracycline resistance determinants: mechanisms of action, regulation of expression, genetic mobility, and distribution, FEMS Microbiol. Rev. 19 (1996) 1–24.